

# Predictions of exclusive $\psi(2S)$ production at the LHC

S.P. JONES<sup>a</sup>, A.D. MARTIN<sup>b</sup>, M.G. RYSKIN<sup>b,c</sup> and T. TEUBNER<sup>a</sup>

<sup>a</sup> *Department of Mathematical Sciences,  
University of Liverpool, Liverpool L69 3BX, U.K.*

<sup>b</sup> *Department of Physics and Institute for Particle Physics Phenomenology,  
University of Durham, Durham DH1 3LE, U.K.*

<sup>c</sup> *Petersburg Nuclear Physics Institute, NRC Kurchatov Institute, Gatchina, St. Petersburg,  
188300, Russia*

## Abstract

The cross section for exclusive  $\psi(2S)$  ultraperipheral production at the LHC is calculated using gluon parametrisations extracted from exclusive  $J/\psi$  measurements performed at HERA and the LHC. Predictions are given at leading and next-to-leading order for  $pp$  centre-of-mass energies of 7, 8 and 14 TeV, assuming the non-relativistic approximation for the  $\psi(2S)$  wave function.

Recently, measurements of exclusive  $J/\psi$  production in ultraperipheral  $pp$  and  $Pb-Pb$  collision have been published by the LHCb and ALICE collaborations, [1, 2]. More data, with better statistics for the  $J/\psi$  and the  $\psi(2S)$  than the published results, are currently being analysed.<sup>1</sup> In this short note, using the framework and gluon parametrisations from [4], we make predictions for the exclusive  $\psi(2S)$  production at the LHC for  $pp$  centre-of-mass energies of  $\sqrt{s} = 7, 8$  and 14 TeV. Alternative predictions for exclusive  $\psi(2S)$  production at the LHC within the dipole formalism are given in Refs. [5, 6].

---

<sup>1</sup> Note added in proof: these data have subsequently been published [3]

For clarity, let us repeat the main formulae used for the leading order (LO) and next-to-leading order (NLO) predictions. The LO photoproduction cross section for  $\gamma p \rightarrow \psi(2S) p$  is driven by the gluon distribution  $xg$  and, in the case of zero  $t$ -channel momentum transfer ( $t = 0$ ), is given by [7]

$$\left. \frac{d\sigma}{dt} (\gamma p \rightarrow \psi(2S) p) \right|_{t=0} = \frac{\Gamma_{ee} M_{\psi(2S)}^3 \pi^3}{48\alpha} \left[ \frac{\alpha_s(\bar{Q}^2)}{\bar{Q}^4} xg(x, \bar{Q}^2) \right]^2, \quad (1)$$

where  $\alpha$  is the QED coupling,  $M_{\psi(2S)}$  is the mass of the  $\psi(2S)$  and  $\Gamma_{ee}$  is its electronic width. For photoproduction the kinematic variables are

$$\bar{Q}^2 = M_{\psi(2S)}^2/4, \quad x = M_{\psi(2S)}^2/W^2, \quad (2)$$

and  $W$  is the  $\gamma p$  centre-of-mass energy. In order to include data integrated over  $t$  we assume the cross section depends exponentially on  $t$ , i.e.  $\sigma \sim \exp(-B|t|)$ . The energy-dependent  $t$  slope parameter,  $B$ , is, given by the Regge motivated form

$$B(W) = (4.9 + 4\alpha' \ln(W/W_0)) \text{ GeV}^{-2}, \quad (3)$$

where the pomeron slope  $\alpha' = 0.06$  and  $W_0 = 90$  GeV, essentially unchanged from the  $J/\psi$  case. Corrections due to the skewing of the gluons and the real part of the amplitude are included as in [4].

At NLO we account for the fact that no additional gluons with transverse momentum larger than  $k_T$  are emitted in the process by including the Sudakov factor

$$T(k_T^2, \mu^2) = \exp \left[ \frac{-C_A \alpha_s(\mu^2)}{4\pi} \ln^2 \left( \frac{\mu^2}{k_T^2} \right) \right] \quad (4)$$

with  $T = 1$  for  $k_T^2 \geq \mu^2$ . Integrating over the  $k_T$  of the gluons, the ‘NLO’ cross section<sup>2</sup> is obtained, as derived in [4], by the replacement

$$\left[ \frac{\alpha_s(\bar{Q}^2)}{\bar{Q}^4} xg(x, \bar{Q}^2) \right] \longrightarrow \int_{Q_0^2}^{(W^2 - M_{\psi(2S)}^2)/4} \frac{dk_T^2 \alpha_s(\mu^2)}{\bar{Q}^2(\bar{Q}^2 + k_T^2)} \frac{\partial \left[ xg(x, k_T^2) \sqrt{T(k_T^2, \mu^2)} \right]}{\partial k_T^2} + \ln \left( \frac{\bar{Q}^2 + Q_0^2}{\bar{Q}^2} \right) \frac{\alpha_s(\mu_{\text{IR}}^2)}{\bar{Q}^2 Q_0^2} xg(x, Q_0^2) \sqrt{T(Q_0^2, \mu_{\text{IR}}^2)}. \quad (5)$$

Here we have assumed the behaviour of  $xg(x, k_T^2) \sqrt{T}$  to be linear in  $k_T^2$  for  $k_T$  below the infrared scale  $Q_0 = 1$  GeV. The scales are chosen to be  $\mu^2 = \max(k_T^2, \bar{Q}^2)$  and  $\mu_{\text{IR}}^2 = \max(Q_0^2, \bar{Q}^2)$ . When evaluating (1) and (5) we use the LO and NLO gluon parametrisations fitted in [4].

Note that for  $\psi(2S)$  the relativistic corrections due to the vector meson wave function may be larger than for the  $J/\psi$ , where they were found to suppress the cross section by about 6%

---

<sup>2</sup>By integrating over the gluon  $k_T$  we account for an important part of the next-to-leading order effects, although we do not include the full set of NLO corrections to the hard matrix element.

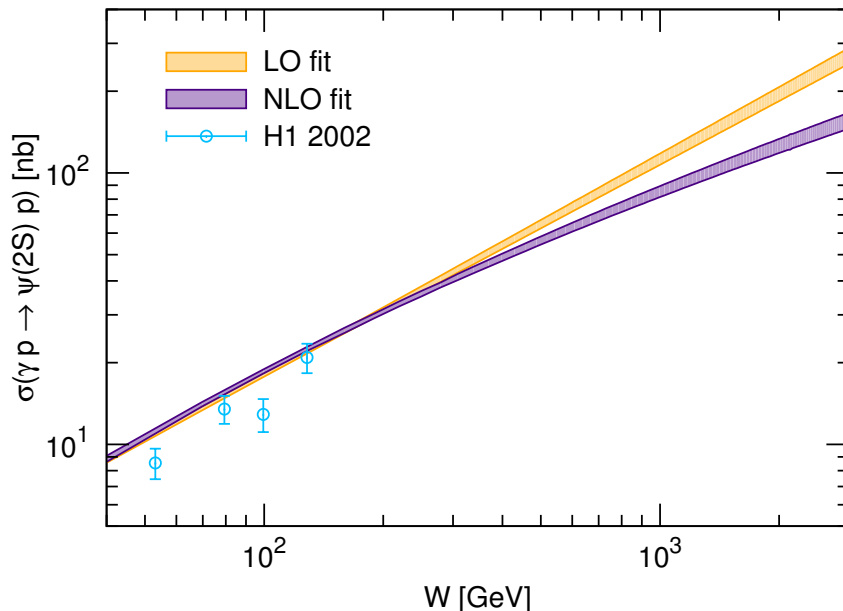


Figure 1: Prediction of exclusive  $\psi(2S)$  photoproduction as a function of the  $\gamma p$  centre-of-mass energy. Also shown, but not fitted, are the available  $\psi(2S)$  data from H1 [9, 10]. The width of the shaded bands indicates only the  $1\sigma$  uncertainty from the  $J/\psi$  experimental data used in the gluon fits.

[8]. While a part of the relativistic corrections related to the wave function at the origin is accounted for using  $\Gamma_{ee}$ , the measured electronic width of the  $\psi(2S)$ , one may expect a further suppression in the case of  $\psi(2S)$  compared to  $J/\psi$ . We do not account for this.

What additional uncertainties are there in our predictions for the gluon distribution? First, there may be an uncertainty arising from the skewed factor which accounts for the difference between the conventional (diagonal) gluon PDF and the generalised (GPD) distribution. As described in [4], we use the Shuvaev transform to relate the diagonal PDF and the GPD. This provides sufficient accuracy,  $\sim \mathcal{O}(x)$ , in our low  $x$  domain. Next, there may be an uncertainty coming from the real part of the amplitude, which is evaluated approximately. Again the corresponding uncertainty is small (less than 2%) in the low  $x$  region, where the  $x$  dependence is not steep and the Re/Im ratio is rather small. We emphasize that the uncertainties, both from the skewed factor and the Re/Im ratio, apply to  $xg(x)$  and *not* to the ratio of the  $\psi(2S)$  to  $J/\psi$  cross sections in which they cancel almost exactly. Thus, the main uncertainty in the  $\psi(2S)$  cross section, calculated using the gluon extracted from the  $J/\psi$  data, is that coming from the relativistic correction for  $\psi(2S)$ .

Figure 1 displays our results for the  $\gamma p \rightarrow \psi(2S)p$  cross section in LO and NLO. The width of the shaded bands gives the  $1\sigma$  uncertainty from the  $J/\psi$  experimental data used in the gluon fits. Note that we do not include the available  $\psi(2S)$  data from H1 [9] in the gluon fit, they are shown just for comparison. The data [9] only gives the values of the ratio of the  $\psi(2S)$  to

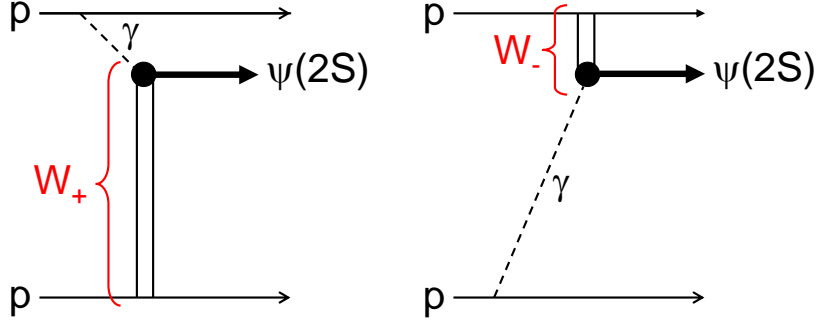


Figure 2: Subprocesses contributing to exclusive  $\psi(2S)$  production in ultraperipheral  $pp$  collisions.  $W_+$  and  $W_-$  are the  $\gamma p$  centre-of-mass energies. The vertical axis corresponds to the  $\psi(2S)$  rapidity.

$J/\psi$  cross sections. To obtain the  $\psi(2S)$  photoproduction data points displayed in Fig. 1 we use the fit  $\sigma_{J/\psi} = 81 (W/90 \text{ GeV})^{0.67} \text{ nb}$  for the  $J/\psi$  cross section obtained by H1 [10]. Our predictions are slightly above the data.

We can now make predictions for exclusive  $\psi(2S)$  production in ultraperipheral  $pp$  collisions as a function of the  $\psi(2S)$  rapidity, using the  $\gamma p \rightarrow \psi(2S) p$  cross section. Note that for a given rapidity  $y$ , two  $\gamma p$  subprocesses with different  $\gamma p$  centre-of-mass energies squared,  $W_{\pm}^2 = M_{\psi(2S)} \sqrt{s} \exp(\pm|y|)$ , and different photon fluxes,  $dn/dk_{\pm}$ , contribute, depending on which of the protons acts as photon emitter and which as target, as illustrated in Fig. 2. In the absence of forward proton tagging these two subprocesses can not be distinguished and must be added, see (6) below.

Recall that our analysis is well justified at small  $x$ ,  $x \lesssim 0.01$ , which provides good accuracy of both the Shuvaev transform, used to relate the diagonal gluons and GPDs, and the real part contribution. Moreover, the simple expression used to parametrize the gluon distribution is not appropriate at large  $x$ . The  $J/\psi$  data included in the gluon fit [4], used in this analysis, contains the low energy  $W_-$  contribution to the LHC data for which the small  $x$  approximation is not justified. In future analyses, it may be better to repeat the gluon fit after subtracting the contribution arising from the low energy  $W_-$  configuration from the LHC  $J/\psi$  ultraperipheral  $pp$  production data. To estimate this contribution a fit to the low energy fixed target data measured at E401 and E516 [11, 12] could be used. This low energy fixed target fit along with a further fit to the ratio of the  $\psi(2S)$  to  $J/\psi$  photoproduction cross sections, measured by H1 [9], would allow the  $W_-$  contribution to  $\psi(2S)$  ultraperipheral  $pp$  production cross sections to be estimated. Note, however, for  $\psi(2S)$  the size of the  $W_-$  contribution is small relative to the  $W_+$  contribution due to the lower photon energy and small low energy photoproduction cross section. Thus, though our theory prediction overestimates the  $W_-$  contribution to the ultraperipheral  $pp$  production its contribution is dominated by the  $W_+$  contribution.

In hadron collisions we also have to take into account additional soft interactions between the colliding hadrons, which can destroy the exclusive signature (rapidity gap) of the event.

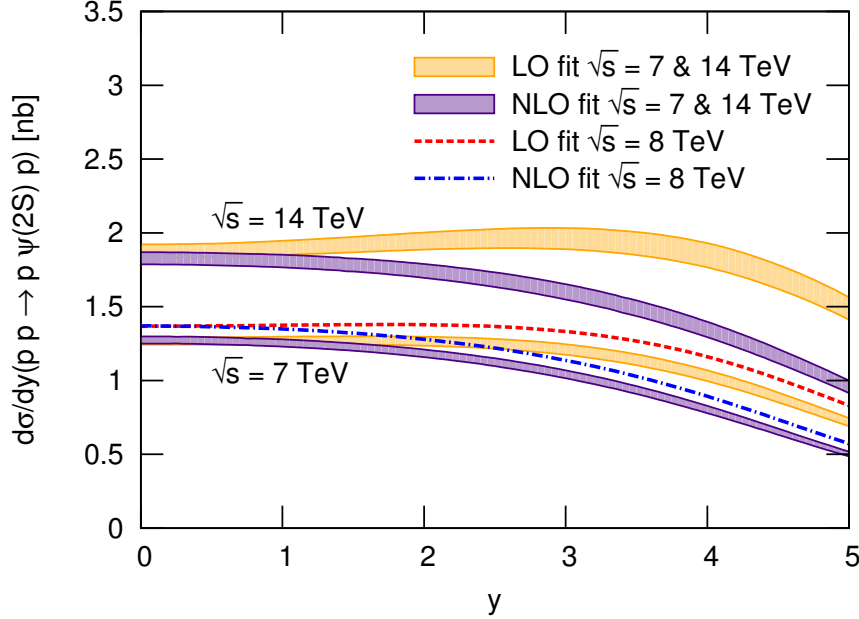


Figure 3: Prediction of the exclusive  $pp \rightarrow p + \psi(2S) + p$  cross section as a function of the  $\psi(2S)$  rapidity  $y$  for  $pp$  centre-of-mass energies  $\sqrt{s} = 7$  and 14 TeV (shaded bands) and  $\sqrt{s} = 8$  TeV (dashed and dash-dotted lines). The width of the shaded bands indicates only the  $1\sigma$  uncertainty from the  $J/\psi$  experimental data used in the gluon fits. The uncertainties of the 8 TeV predictions are very similar to the ones shown for 7 TeV and are not displayed.

The necessary gap survival factors for  $\psi(2S)$  production are calculated using the two-channel eikonal model from [13]. They are displayed in Table 1 for the three different  $pp$  centre-of-mass energies of 7, 8 and 14 TeV and for a large range of rapidities as relevant for the LHC experiments. The columns labelled  $S^2(W_+)$  and  $S^2(W_-)$  give the suppression factors for the two different  $\gamma p$  energies  $W_{\pm}$  as a function of rapidity for each  $pp$  centre-of-mass energy.

Our theoretical prediction for the exclusive  $\psi(2S)$  production in ultraperipheral  $pp$  collisions,  $d\sigma(pp)/dy$ , in terms of our exclusive photoproduction cross sections,  $\sigma_{\pm}(\gamma p)$ , for the two subprocesses  $\gamma p \rightarrow \psi(2S)p$  at energies  $W_{\pm}$  is therefore given by

$$\frac{d\sigma(pp)}{dy} = S^2(W_+) \left( k_+ \frac{dn}{dk_+} \right) \sigma_+(\gamma p) + S^2(W_-) \left( k_- \frac{dn}{dk_-} \right) \sigma_-(\gamma p). \quad (6)$$

The photon energies are given by  $k_{\pm} \approx (M_{\psi(2S)}/2) \exp(\pm|y|)$  and the photon fluxes are calculated as described in [4]. Our cross section predictions are shown in Fig. 3 for the three  $pp$  centre-of-mass energies of 7, 8 and 14 TeV. As in Fig. 1, the bands only indicate the experimental uncertainty of the gluon fit parameters used for the LO and NLO predictions.

In summary, following and supplementing [4], we have predicted the cross section for exclusive  $\psi(2S)$  production in ultraperipheral  $pp$  collisions at the LHC, using gluon parametrisations extracted from HERA and LHC exclusive  $J/\psi$  production data. In principle, once precise  $\psi(2S)$

data become available, they could be included in a combined analysis, together with  $J/\psi$  and possibly  $\Upsilon$  data. Such an analysis, depending on the accuracy of the data, will require a more detailed understanding of the relativistic corrections from the vector meson wave functions and would benefit from a complete next-to-leading order prediction of the underlying elastic vector meson production process,  $\gamma p \rightarrow V p$ , which is beyond the scope of this paper.

## Acknowledgements

We thank Ronan McNulty for interesting discussions and for encouraging us to make these predictions. MGR thanks the IPPP at the University of Durham for hospitality. This work was supported by the grant RFBR 14-02-00004 and by the Federal Program of the Russian State RSGSS-4801.2012.2.

## References

- [1] R. Aaij *et al.* [LHCb Collaboration], J. Phys. G **40** (2013) 045001, [arXiv:1301.7084 \[hep-ex\]](#).
- [2] B. Abelev *et al.* [ALICE Collaboration], Phys. Lett. B **718** (2013) 1273, [arXiv:1209.3715 \[nucl-ex\]](#).
- [3] R. Aaij *et al.* [LHCb Collaboration], [arXiv:1401.3288](#).
- [4] S.P. Jones, A.D. Martin, M.G. Ryskin and T. Teubner, JHEP **11** (2013) 085, [arXiv:1307.7099 \[hep-ph\]](#).
- [5] M.B. Gay Ducati, M.T. Griep and M.V.T. Machado, Phys. Rev. D **88** (2013) 017504, [arXiv:1305.4611 \[hep-ph\]](#).
- [6] M.B. Gay Ducati, M.T. Griep and M.V.T. Machado, Phys. Rev. C **88** (2013) 014910, [arXiv:1305.2407 \[hep-ph\]](#).
- [7] M.G. Ryskin, Z. Phys. C **57** (1993) 89.
- [8] P. Hoodbhoy, Phys. Rev. D **56** (1997) 388, [\[hep-ph/9611207\]](#).
- [9] C. Adloff *et al.* [H1 Collaboration], Phys. Lett. B **541** (2002) 251, [arXiv:hep-ex/0205107](#).
- [10] C. Alexa *et al.* [H1 Collaboration], Eur. Phys. J. C **73** (2013) 2466, [arXiv:1304.5162 \[hep-ex\]](#).

- [11] M. Binkley *et al.*, Phys. Rev. Lett. **48** (1982) 73
- [12] B. Denby *et al.*, Phys. Rev. Lett. **52** (1984) 795
- [13] V.A. Khoze, A.D. Martin and M.G. Ryskin, Eur. Phys. J. C **73** (2013) 2503,  
[arXiv:1306.2149](#) [hep-ph].

	7 TeV		8 TeV		14 TeV	
$y$	$S^2(W_+)$	$S^2(W_-)$	$S^2(W_+)$	$S^2(W_-)$	$S^2(W_+)$	$S^2(W_-)$
0.125	0.858	0.864	0.860	0.865	0.867	0.871
0.375	0.853	0.869	0.855	0.870	0.862	0.875
0.625	0.846	0.873	0.848	0.875	0.856	0.879
0.875	0.839	0.878	0.842	0.879	0.851	0.883
1.125	0.832	0.882	0.835	0.883	0.845	0.887
1.375	0.824	0.885	0.827	0.886	0.838	0.890
1.625	0.815	0.889	0.818	0.890	0.831	0.893
1.875	0.805	0.892	0.809	0.893	0.823	0.896
2.125	0.794	0.895	0.798	0.896	0.814	0.899
2.375	0.782	0.898	0.787	0.899	0.804	0.902
2.625	0.768	0.901	0.774	0.902	0.794	0.904
2.875	0.753	0.904	0.759	0.904	0.782	0.906
3.125	0.736	0.906	0.743	0.907	0.769	0.909
3.375	0.717	0.909	0.725	0.909	0.754	0.911
3.625	0.696	0.911	0.705	0.911	0.738	0.913
3.875	0.673	0.913	0.683	0.913	0.720	0.915
4.125	0.649	0.915	0.659	0.915	0.700	0.917
4.375	0.624	0.917	0.634	0.917	0.677	0.919
4.625	0.600	0.919	0.609	0.919	0.653	0.920
4.875	0.582	0.921	0.588	0.921	0.628	0.922
5.125	0.573	0.922	0.573	0.923	0.602	0.924
5.375	0.581	0.924	0.571	0.924	0.580	0.925
5.625	0.611	0.926	0.590	0.926	0.563	0.927
5.875	0.666	0.927	0.632	0.927	0.559	0.928

Table 1: Rapidity gap survival factors  $S^2$  for exclusive  $\psi(2S)$  production,  $pp \rightarrow p + \psi(2S) + p$ , as a function of the  $\psi(2S)$  rapidity  $y$  for  $pp$  centre-of-mass energies of 7, 8 and 14 TeV. The columns labelled  $S^2(W_{\pm})$  give the survival factors for the two independent subprocesses at different  $\gamma p$  centre-of-mass energies  $W_{\pm}$ .